eIF1A augments Ago2-mediated Dicer-independent miRNA biogenesis and RNA interference

HHS Public Access

Author manuscript

Nat Commun. Author manuscript; available in PMC 2015 November 28.

Published in final edited form as:

Nat Commun. ; 6: 7194. doi:10.1038/ncomms8194.

eIF1A augments Ago2-mediated Dicer-independent miRNA biogenesis and RNA interference

Tingfang Yi[1,*], **Haribabu Arthanari**[1,*], **Barak Akabayov**[1,5], **Huaidong Song**[2], **Evangelos Papadopoulos**[1], **Hank H. Qi**[3], **Mark Jedrychowski**[4], **Thomas Güttler**[4], **Cuicui Guo**[2], **Rafael E. Luna**[1], **Steven P. Gygi**[4], **Stephen A. Huang**[2], and **Gerhard Wagner**[1]

[1]Department of Biological Chemistry and Molecular Pharmacology, Harvard Medical School, 240 Longwood Avenue, Boston, MA 02115 USA

[2]Department of Pediatrics, Children's Hospital Boston, Boston, MA 02115 USA

[3]Department of Anatomy and Cell Biology, University of Iowa Carver College of Medicine, Iowa City, IA 52242 USA

[4]Department of Cell Biology, Harvard Medical School, 240 Longwood Avenue, Boston, MA 02115 USA

[5]Department of Chemistry, Ben-Gurion University of the Negev, Be'er-Sheva 84105, Israel

Abstract

MicroRNA (miRNA) biogenesis and miRNA-guided RNA interference (RNAi) are essential for gene expression in eukaryotes. Here we report that translation initiation factor eIF1A directly interacts with Ago2 and promotes Ago2 activities in RNAi and miR-451 biogenesis. Biochemical and NMR analyses demonstrate that eIF1A binds to the MID-domain of Ago2 and this interaction does not impair translation initiation. Alanine mutation of the Ago2-facing Lys56 in eIF1A impairs RNAi activities in human cells and zebrafish. The eIF1A-Ago2 assembly facilitates Dicer-independent biogenesis of miR-451, which mediates erythrocyte maturation. Human eIF1A (heIF1A), but not heIF1A(K56A), rescues the erythrocyte maturation delay in *eif1axb* knockdown zebrafish. Consistently, miR-451 partly compensates erythrocyte maturation defects in zebrafish with *eif1axb* knockdown and eIF1A(K56A) expression, supporting a role of eIF1A in miRNA-451 biogenesis in this model. Our results suggest that eIF1A is a novel component of the Ago2-centered RNA induced silencing complexes (RISCs) and augments Ago2-dependent RNAi and miRNA biogenesis.

Correspondence: G.W. (Gerhard_Wagner@hms.harvard.edu).

*These authors contributed equally to this work.

Author contributions

T.F.Y., H.A. and G.W. designed and conceived the study. T.F.Y. performed experiments. H.A. and T.F.Y. performed HSQC assays. B.A. and T.F.Y performed miRNA biogenesis and RNAi *in vitro* assays. H.D.S, T.F.Y. and C.C.G. performed zebrafish experiments. M.J. did mass-spectrometric assay. T.F.Y. and H. H. Q. performed GFP reporter assays. E.P. and T.F.Y. analyzed the interaction between eIF1A and Ago2 fragments. T.G and Y.T.F performed polysome profiling assays. All authors contributed to the final version of the paper. The manuscript was written by T. F.Y., H.A. and G.W.

Competing financial interests: The authors declare no competing financial interests.

microRNAs (miRNAs) are ~22 nucleotide (nt) endogenous noncoding RNAs involved in gene expression regulation. Their genes are usually transcribed by RNA polymerase II or III[1,2]. The resulting primary miRNAs (priRNAs) contain characteristic hairpins, which are excised in the nucleus by Drosha/DGCR8 to yield the pre-miRNAs[3,4]. Subsequently, the Exportin-5/Ran-GTP complex translocates the pre-miRNAs to the cytoplasm[5,6], where they are engaged by DICER to form a RISC Loading Complex (RLC). RLC includes TRBP and Ago2[7–9], while ADAR1 facilitates pre-miRNA loading[10]. In the canonical miRNA biogenesis pathway, DICER removes the terminal loop region to yield the mature miRNA[11–13]. Recent studies revealed that miR-451 is produced by an alternative DICER-independent pathway, where pre-miR-451 is loaded directly onto Ago2 and sliced on the 3′ hairpin arm, as guided by the 5′ end of the hairpin, yielding a 30nt cleaved species[14–16]. A 3′ resection activity by PARN trims ~ 7-nt to produce the 23-nt miR-451[17]. However, the mechanisms of DICER-independent miRNA biogenesis have remained elusive.

miRNAs are incorporated into effector ribonucleoprotein complexes called RNA induced silencing complexes (RISCs) to exert RNA interference. RISCs can suppress translation without mRNA degradation, destabilize mRNAs by deadenylation or directly degrade mRNAs by Ago2 slicer activity[12,18–20], and inhibit translation at the stage of initiation or elongation[21,22]. The core of RISCs is a member of the Ago protein family[23]. In mammals, this family consists of four members (Ago1–4). Although these four Ago proteins can suppress translation of their target mRNAs, only Ago2 (also known as eIF2C2) is endonucleolytically active[19,20]. Ago2 is composed of four globular domains (N, PAZ, MID and PIWI) and two structured linker domains (L1 and L2)[24]. MID and PAZ domains harbor the 5′-phosphate and 3′-hydroxyl termini of miRNA, respectively[25,26], while the PIWI domain is responsible for the cleavage—slicer—activity[27,28]. Crystal structures of human Ago2 revealed that the 5′-end of miRNA is tethered to Argonaute through interactions with a binding pocket that is mostly formed by the MID domain[29,30].

Eukaryotic translation initiation factor eIF1A is composed of a globular domain (GD) and two unstructured tails (N- and C-terminal tail), which are absent in prokaryotic initiation factor-1 (IF1). The eIF1A globular domain consists of an IF homologous oligonucleotide/oligosaccharide binding (OB) fold, and an additional subdomain C-terminal to the OB fold that contains two alpha helices and two extended strands, which pack to the helix on opposite sites. The globular domain contains a large RNA binding face[31], which is directed towards the ribosome [32,33]

Here we find that the GD of eIF1A, which is conserved from IF1 to eIF1A, directly binds to Ago2, and that the MID-domain of Ago2 interacts with eIF1A but does not affect eIF1A's function in translation initiation. eIF1A forms a complex with Ago2 and promotes Ago2 cleavage activity in RNAi, and enhances Ago2 activity in miR-451 production in human cells and the developing zebrafish. The results support the notion that eIF1A is a component of the Ago2-centered RISCs.

Results

eIF1A interacts with Ago2

To identify new components of the protein networks that participate in DICER-independent miRNA biogenesis and Ago2-mediated RNAi, we generated a human embryonic kidney 293 (HEK293) cell line that stably expresses Flag-HA (haemagglutinin)-Ago2 for immunoprecipitation analyses. Eukaryotic translation initiation factor eIF1A is a previously unrecognized Ago2-interaction protein that is immunoprecipitated by Ago2 in cell lysates and colocalizes with Ago2 in mammalian cells (Fig. 1a–b). To test the specificity of the eIF1A–Ago interaction, we tested for possible interactions with other members of the Ago family using HEK293 cells stably expressing Ago 1–4[34]. Transiently overexpressed eIF1A showed interaction with Ago2, but not Ago1, Ago3 or Ago4 (Fig. 1c).

eIF1A binds to Ago2 in an RNA-independent manner

To identify which of the individual domain(s) of Ago2 interacts with eIF1A, we examined the interaction of recombinant—RNase A and Benzonase-treated—L1, PAZ, MID and PIWI domains of Ago2 with GST-tagged-eIF1A in pull down assays. RNA free eIF1A specifically interacted with the RNA free MID-domain (Fig. 2a and Supplementary Fig. 1a). To further characterize the interaction between human eIF1A fragments and Ago2, we screened recombinant GST-tagged eIF1A and eIF1A mutants (N-tail deletion, C-tail deletion, and globular domain, Supplementary Fig. 1b–c) for interaction with Ago2. GST-tagged full length, N-tail deletion (ND), C-tail deletion (CD) and globular domain (GD) of eIF1A interacted with Ago2 but not the GST-tag alone, indicating that the eIF1A-GD is required and sufficient for the interaction with Ago2 (Fig. 2b). We further investigated the interaction between RNase A and Benzonase-treated eIF1A and the MID-domain by Nuclear Magnetic Resonance (NMR) spectroscopy. Unlabeled, Sumo-tagged MID domain titrated into a ^{15}N-labeled sample of eIF1A at molar ratio of 1:1 (eIF1A:SMT3-MID) (Fig. 2c) resulted in broadening of eIF1A resonances characteristic of the complex being in an intermediate exchange regime. The resonances of the eIF1A-GD experience more broadening when compared to the unstructured tails. For instance, resonances of Val55, Lys56 and Lys67 residues of ^{15}N-eIF1A-GD show broadening upon MID domain titration (Fig. 2c). These results suggest that the interaction of eIF1A and Ago2 primarily involves the GD of eIF1A. Furthermore, when unlabeled RNA free eIF1A was titrated to the RNA free ^{15}N-MID-domain at molar ratio of 1:1, we observed broadening of the MID resonances indicative of direct binding between the two proteins (Fig. 2d). We verified that eIF1A does not bind to the SMT3-tag (strong signals in Fig. 2d). These NMR data demonstrate that eIF1A directly interacts with Ago2 in an RNA independent manner.

Ago2 interaction does not impair eIF1A translation functions

Based on the observed spectral changes (Fig. 2c) we generated three eIF1A mutants: V55A, K56A and K67A. To test whether the mutants are folded we recorded a TROSY HSQC spectrum of eIF1A^{K56A}. The spectrum clearly shows that eIF1A^{K56A} is properly folded (Supplementary Fig. 2). To examine the roles of Val55, Lys56 and Lys67 of eIF1A in full length eIF1A-Ago2 interaction, we generated HEK293 cell lines stably expressing single eIF1A mutants (V55A, K56A or K67A) involved in Ago2-eIF1A interaction. As determined

by immunoprecipitation, all three mutations reduced eIF1A-Ago2 interaction (Fig. 3a), suggesting that these amino acids in eIF1A are important for the interaction between Ago2 and full-length eIF1A. In an *in vitro* dual luciferase translation assays, elevated eIF1A^{K56A} increases cap-dependent and IRES-dependent translation, to a similar degree as wild type eIF1A (Fig. 3b), suggesting that the K56A mutation does not compromise the activity of eIF1A in translation initiation. In addition, eIF1A^{K56A} does not repress polysome complex formation activities in polysome profiling analyses (Fig. 3c), indicating that the K56A mutation does not generally impair translation.. Taken together, the data suggests that eIF1A directly interacts with Ago2 in an RNA-binding-independent manner, the MID-domain of Ago2 binds to the GD of eIF1A, and that the interaction between eIF1A and Ago2 does not impair eIF1A functions in translation initiation.

eIF1A promotes Ago2-mediated miRNA-guided RNAi *in vitro*

To examine whether eIF1A plays a role in Ago2-mediated RNAi, we employed a human *HMGA2* 3′-UTR mutant which harbors a characterized native let-7 target site[35] (Fig. 4a). This assay evaluates the dependence of eIF1A and its mutants on let-7a/Ago2 mediated cleavage of the target mRNA. In the RNAi *in vitro* assay reactions with added eIF1A or eIF1A mutants without Ago2, no cleavage product was observed, suggesting that the cleavage is Ago2 dependent (Fig. 4b). Interestingly, we found that high concentrations of eIF1A increased *HMGA2* 3′-UTR mutant cleavage while eIF1A mutants (V55A, K56A and K67A) significantly reduced the level of cleavage products (Fig. 4b–c), indicating that eIF1A augments Ago2-mediated RNAi activities *in vitro*. To investigate the effects of eIF1A in Ago2-mediated miRNA-guided RNAi activities in cells, we used green fluorescent protein (GFP) reporters containing let-7 targeted sequences[36]. Because transient knockdown of eIF1A in HEK293 cells led to significant decrease of cell viability (Supplementary Fig. 3), we employed specific eIF1A-Ago2 interaction interference with eIF1A^{K56A}. Increased eIF1A levels elevated let-7 RISC activity, while eIF1A (K56A) mutant compromised let-7 RISC activity (Fig. 4d–e). Elevated eIF1A and Ago2 decrease cellular *GFP* mRNA levels as determined by qPCR (Fig. 4f). In contrast, eIF1A^{K56A} caused increased cellular *GFP* mRNA levels (Fig. 4f). These results suggest that eIF1A forms a complex with Ago2 and promotes Ago2-mediated RNAi in human cells *in vitro*.

eIF1A promotes Ago2-mediated miRNA-guided RNAi *in vivo*

To further evaluate the roles of eIF1A on Ago2-mediated RNAi in an animal model, we employed zebrafish. Both zebrafish paralog eIF1AXa and eIF1AXb interact with Ago2 (Supplementary Fig. 4a–b). *eif1axb* mRNA level is much higher (> 25-fold) than that of *eif1axa* in the developing zebrafish (Supplementary Fig. 4c–d) therefore we focused on eif1axb here. We employed a lower dosage of *eif1axb* Morpholino (MO, 62.5μM, 1nl), which does not significantly affect zebrafish phenotypes at 18 h.p.f and 48 h.p.f (Supplementary Fig. 4e–f). Previous studies reported that miR-126 targets *c-Myb* and suppresses c-Myb expression in zebrafish[37]. We next examined if eIF1A plays a role in Ago2-mediated miR-126-guided c-Myb suppression in zebrafish at 28 h.p.f. Zebrafish treated with *eif1axb* MO (62.5μM, 1nl) showed increased c-Myb in comparison to the control group (Fig. 4g). Zebrafish with treatment of *eif1axb* MO (62.5μM, 1nl) plus human eIF1A (heIF1A, 1μg/μl mRNA, 1nl) presented decreased c-Myb levels compared to the

group treated with only *eif1axb* MO (62.5μM, 1nl). In contrast, zebrafish treated with human eIF1A^{K56A} (1μg/μl mRNA, 1nl) and *eif1axb* MO (62.5μM, 1nl) show increased c-Myb (Fig. 4g). In addition, heIF1A^{K56A} increased *c-Myb* mRNA accumulation in zebrafish (Fig. 4h), indicating that interfering with eIF1A-Ago2 interaction impairs the miR-126-mediated suppression of *c-Myb* expression in zebrafish, even though the level of miR-126 remain is not significantly decreased under these conditions (Fig. 4i). These results demonstrated that eIF1A-Ago2 complex promotes miR-126 RISC activities *in vivo*. Overall the above results demonstrate that eIF1A augments Ago2-mediated miRNA-guided RNAi both *in vitro* and *in vivo*.

eIF1A stimulates miR-451 biogenesis *in vitro* and *in vivo*

Ago2 is important for Dicer-independent generation of mature miR-451, a micro RNA that regulates erythropoiesis [14–16]. We therefore investigated whether eIF1A is involved in Ago2-mediated DICER-independent miRNA biogenesis. *In vitro* analyses of eIF1A/Ago2-dependent cleavage of pre-miR-451 showed that reactions with eIF1A or eIF1A mutants but without Ago2 displayed no pre-miR-451 cleavage (Fig. 5a). In the presence of Ago2, however, eIF1A enhances pre-miR-451 cleavage in a dose-dependent manner (Fig. 5a–b). In contrast, the point mutation of V55A, K56A or K67A impaired the activity of Ago2 in this assay (Fig. 5a–b). These results suggest that eIF1A forms a complex with Ago2 to facilitate pre-miR-451cleavage. In Northern blot assays, eIF1A mutants (V55A, K56A, or K67A) in stable HEK293 cells consistently decreased the production or accumulation of mature miR-451 in comparison to wild type eIF1A (Fig. 5c). Importantly, the level of miR-144—which is processed from the same precursor transcript as miR-451[14,15]—remained unchanged (Fig. 5c). These results suggest that eIF1A promotes Ago2-dependent miR-451 biogenesis in human cells *in vitro*. While the levels of miRNA-451 increased during development from 24 h.p.f. to 56 h.p.f in wild type zebrafish, *eif1axb* knockdown lead to decreased miR-451production (Fig. 5d). Human eIF1A (1μg/μl mRNAs, 1nl) could rescue miR-451 production in *eif1axb* knockdown zebrafish (Fig. 5d). In contrast, heIF1A^{K56A} failed to rescue miR-451 production during zebrafish development (Fig. 5d), indicating that eIF1A-Ago2 interaction plays a role in miR-451 biogenesis *in vivo*. Importantly, *eif1axb* knockdown does not decrease miR-144 production, indicating that eIF1A does not affect Ago2-independent miRNA production (Fig. 5d). These results demonstrated that eIF1A forms a complex with Ago2 and augments Ago2-dependent miR-451 biogenesis in zebrafish.

eIF1A modulates miR-451 mediated erythrocyte maturation

Recent studies have reported that miR-451 plays an important role in erythrocyte maturation in zebrafish[15,38,39]. Consistent with a role for eIF1A in miR-451 biogenesis, injection of human *eIF1A* mRNAs (1μg/μl, 1nl, n = 35 embryos), but not mRNAs encoding human eIF1A^{K56A} (1μg/μl, 1nl, n = 35), rescues the reduced hemoglobinized cells in zebrafish with *eif1axb* gene knockdown (Fig. 5e–f). Importantly, miR-451 (0.2μg/μl, 1nl, n = 31) partly compensated the decrease in hemoglobinized cells in zebrafish treated with *eif1axb* knockdown or heIF1A^{K56A} (Fig. 5e–f). Furthermore, heIF1A (n = 120 erythrocytes), but not heIF1A^{K56A} mutant (n = 145 erythrocytes), rescued erythrocyte maturation in zebrafish with *eif1axb* knockdown. Notably, miR-451 (0.2μg/μl, 1nl, n = 118 erythrocytes) rescued

erythrocyte maturation delay caused by heIF1A^{K56A} expression (Fig. 5g–h). These results demonstrate that eIF1A modulates miR-451 production in zebrafish. Taken together, our data demonstrate that eIF1A forms a complex with Ago2 and promotes Ago2-mediated miRNA-guided RNAi and Ago2-dependent Dicer-independent miRNA biogenesis.

Discussion

Ago2-mediated miRNA biogenesis and processing are essential for the development in eukaryotes. We found that eIF1A directly binds to Ago2 in an RNA-independent manner, and plays a role in both Ago2-mediated miRNA-guided RNAi and miRNA biogenesis (Fig. 6). Using biochemistry and NMR analyses, we demonstrated that MID-domain of Ago2 binds to the globular domain of eIF1A. eIF1A promotes Ago2-mediated RNAi and miR-451 biogenesis *in vitro* and *in vivo*. eIF1A augments erythrocyte maturation in zebrafish through mediating miR-451 surveillance. The previously unrecognized roles of eIF1A in Ago2-mediated miRNA processes identified here provide insights into the understanding of the mechanisms of miRNA-guided RNAi and miRNA biogenesis.

Interestingly, point mutation of K56A in eIF1A leads to dissociation of eIF1A-Ago2 interaction. The eIF1A (K56A) mutant does not impair translation initiation. In contrast, eIF1A(K56A) impairs Ago2-mediated miRNA guided RNAi and Ago2-dependent miR-451 production *in vitro* and in zebrafish *in vivo*. Consistently, miR-451 partly reverts reduced hemoglobinization and delayed maturation of erythrocytes in *eif1axb* knockdown zebrafish with overexpressed heIF1A (K56A). These data demonstrate that eIF1A-Ago2 interaction promotes Ago2-mediated RNAi and miRNA production but does not compromise eIF1A functions in translation initiation.

Recently, groups of Ameres et al.[40], Cheloufi et al.[14], and Cifuentes et al.[15] have reported that recombinant Ago2 is sufficient for slicer activity with large quantities of RNA fragments in RNAi and miR-451 processing *in vitro*. These data elegantly evidenced that Ago2 is a central effector of miR-451 generation and RNAi processes. On the other hand, many studies demonstrated that the Ago2-centered RISC complex is necessary for efficient RNAi activity with long and/or structured mRNAs and miR-451 processing *in vivo*[23,41]. It is possible that other components in RISC are needed to resolve mRNA secondary structure, to scan the long and/or structured mRNAs for recognition of miRNA seed regions in low abundance, and to generate mature miR-451. Currently, the component list of RISC is increasing. Here we show that eIF1A directly binds to Ago2 and augments miR-451 biogenesis and RNAi processes, suggesting that eIF1A is an important but previously unrecognized factor of RISC.

MID-domain of Ago2 is essential for miRNA docking in RISC mediated RNAi and pre-miR-451 loading in Dicer-independent miR-451 biogenesis. Here, we found that eIF1A directly binds to MID-domain of Ago2 and eIF1A promotes miRNA-guided RNAi and miR-451 generation.

Our findings reveal that eIF1A directly interacts with Ago2 and augments Ago2-mediated miRNA-guided RNAi and DICER-independent miRNA biogenesis. The newly identified

eIF1A–Ago2 complex together with its functions in miRNA processes provides insights in understanding how Ago2 mediates miRNA processes in translation, development and diseases.

Methods

Plasmids, antibodies and reagents

Constructs of human Flag-HA-Ago1(10820), Ago2 (10822) Ago3 (10823) and Ago4 (10824) were obtained from Addgene. The cDNAs of human eIF1A were PCR-amplified from HEK293 cDNAs. Human eIF1A was inserted into NotI/EcoRI sites of the pIRESneo vector. Mutants of eIF1A: N-tail deletion (ND, 25~144aa, amino acid), C-tail deletion (CD, 1~114aa), globular domain (GD, 25~114aa) were generated by PCR and inserted into NotI/EcoRI sites of the pIRESneo vector encoding an N-terminal with Flag-HA. Monoclonal anti-Flag (#8146S) antibody (20μl for immunoprecipitation assay), monoclonal anti-HA antibody (6E2, 2367S, 20μl for immunoprecipitation assay) and monoclonal anti-GFP antibody (#2956S, 20μl for immunoprecipitation assay, 1:1000 dilution for Western blot assay), and anti-β-Tubulin (2146S, 1:1000 dilution for Western blot assay) were ordered from Cell Signaling. Monoclonal anti-eIF1A antibody (Ab172623, 20μl for immunoprecipitation assay; 1:1000dilution for western blot assay), monoclonal anti-human Ago2 antibody (ab57113, used to detect human and zebrafish Ago2, 1:1000 dilution in western blot assay, 20μl for immunoprecipitation assay), and polyclonal anti-actin (ab1801, for zebrafish actin detection with 1:1000 dilution in Western blot assay) were bought from Abcam. Polyclonal anti-Ago1 (SAB4200065, 1:1000 dilution in Western blot assay) and Ago3 (SAB4200112, 1:1000 dilution in Western blot assay) antibodies were purchased from Sigma. Polyclonal anti-Ago4 antibody (MABE139, 1:1000 dilution in Western blot assay) was ordered from Millipore. Ribonuclease A was ordered from Sigma. Benzonase nuclease was ordered from VWR. HEK293 (CRL-1573™), HeLa (CCL-2™) and T98G (CRL-1690™) cells were ordered from ATCC. SilverXpress® Silver Staining Kit was purchased from Invitrogen. CellTiter-Glo® Luminescent Cell Viability Assay Kit was bought from Promega.

Immunoprecipitation, MS and Western blot assays

The stable HEK293 cell line expressing Flag-HA (as a control) or Flag-HA-Ago2 were lysed with lysis buffer containing 20mM Tris HCl *p*H7.4, 137mM NaCl, 10% glycerol, 1% NP-40, EDTA- free protease inhibitor (Roche) followed by 10μg/ml Ribonuclease A treatment (25°C, 1hr). The Ago2 interacted proteins were immunoprecipitated by anti-HA monoclonal antibodies (Cell Signaling, 2367S, 20μl for immunoprecipitation assay) immobilized to Dyna beads. The purified proteins were analyzed by silver staining and Mass Spectrometry via LC-MS/MS on an LTQ Orbitrap Velos mass spectrometer (Thermo Scientific, German) equipped with a Thermo Fisher Scientific nanospray source, an Agilent 1100 Series binary HPLC pump, and a Famos autosampler. The spectral data were searched with SEQUEST against a database containing the human International Protein Index (IPI) protein sequence database: (http://www.ebi.ac.uk/IPI/) together with the reversed complement. eIF1A was transiently overexpressed in stable HEK293 cell lines expressing Agos (Ago1~ 4). The cell lysates were treated with 10μg/ml Ribonuclease A (25°C, 1hr).

Immunoprecipitated proteins by anti-eIF1A monoclonal antibodies (Abcam, Ab172623, 20μl for immunoprecipitation assay) were analyzed by western blotting with anti-Agos (1~4) antibodies (monoclonal anti-Ago2 antibodies, Abcam, ab57113, 1:1000 dilution; polyclonal anti-Ago1/3, Sigma, SAB4200065, SAB4200112, 1:1000 dilution); Ago4 Millipore, MABE139, 1:1000 dilution)antibodies in immunoblotting (IB).

Expression and purification of eIF1A and Ago2 fragments

The cDNA for MID-domain of human Ago2 (His-Sumo-tagged) was provided by Bhushan Nagar (McGill University). Human eIF1A and mutants of eIF1A-ND/-CD/-GD were inserted into EcoRI/NotI sites of pGEX-4E-1 vectors with GST fusion at the N-term. Human Ago2 (full length) and fragments of L1(172 ~ 227aa), PAZ(227 ~ 349aa), MID (432 ~ 575aa) and PIWI (590 ~ 816aa) were inserted into NdeI/BamHI sites of a pET-6H2 vector. His-tagged proteins expressed in BL21(DE3) cells were extracted by sonication with lysis buffer (50mM Tris, 350mM NaCl, 10mM Imidazole, *p*H8.0, 20μM Benzonase nuclease, 10μg/ml RNase A, 100μg/ml lysozyme, 2% NP-40, 0.05% β-mercaptoethanol and protease inhibitor) followed by Ni-agarose resin (Qiagen) purification. GST-tagged proteins expressed in BL21(DE3) cells were extracted by MagneGST™ Protein Purification System (Promega) or Pierce Glutathione Magnetic Beads (Thermo Scientific).

GST-pull down assays

E. coli expressed GST-tagged human eIF1AX (known as eIF1A), or globular domain (GD, 25 ~114aa), or N-tail deletion (ND, 25~144aa) or C-tail deletion (CD, 1~114aa) were purified by GST-pull down assays (#88822, Thermo Scientific) with glutathione magnetic beads from pre-cleared cell lysates of HEK293 cells stably expressing HA-Ago2 in the presence of 10μg/ml Ribonuclease A treatment. Western blot assays were performed with anti-Ago2 monoclonal antibodies (Abcam, ab57113, 1:1000 dilution). For the Ago2 domain screening assays, *E. coli* expressed His-tagged L1, PAZ, sumo-MID, PIWI domains and Sumo, which were purified by Ni-NTA resin, were performed GST-pull down assays with *E. coli* expressed GST-eIF1A. Western blot assays were performed with anti-His monoclonal antibodies (Cell Signaling, #2366S, - 1:1000 dilution).

Nuclear Magnetic Resonance (NMR) titrations

BL21(DE3) bacterial cells harboring His-SMT3, His-SMT3-tagged MID(432 ~ 575aa) and His-tagged eIF1A grown in either LB or minimal media containing ^{15}N Ammonium Chloride. The resulting cell pellets were lysed by sonication or french press with lysis buffer (50mM Tris, 350mM NaCl, 10mM Imidazole, *p*H8.0, 20μM Benzonase nuclease, 10μg/ml RNase A, 100μg/ml lysozyme, 2% NP-40, 0.05% β-mercaptoethanol, protease inhibitor). The soluble proteins were loaded onto a Ni-agarose resin (Qiagen) and proteins were eluted with Ni-elution buffer (50mM Tris, 350mM NaCl, 350mM Imidazole, *p*H8.0). Purified proteins in Ni-elution buffer were further purified by size exclusion chromatography using a S75 column and eluting with HEPES buffer (20mM HEPES, 150mM NaCl, 0.5mM TCEP, *p*H7.2). The HSQC measurements were carried out on a Bruker 500 MHz and Varian 600 MHz instrument each equipped with a cryogenically cooled probe. The data was processed using NMRPipe and visualized using CARA. The molar ratios of ^{15}N-eIF1A: SMT3-MID at

1:1 were analyzed in this study and the concentration of ^{15}N-eIF1A was at 200μM. Similarly ^{15}N-SMT3-MID was held at concentration of 200μM and unlabeled eIF1A was titrated at molar ratio of 1:1.

Ago2-mediated RNAi and miR-451 biogenesis *in vitro* assays

Target miRNA cleavage analyses[14,15] for Ago2 proteins were performed. Briefly, overexpressed HA-Ago2, HA-eIF1A, HA-eIF1A mutants (V55A, K56A, K67A) proteins were purified with anti-HA antibodies and Dyna beads (Invitrogen) from HEK293 cells via native methods. For the *in vitro* miRNA mediated RNA slicing assays, 100μM let-7a (Dharmacon) and linearized 5μM 5′-^{32}P end-labeled synthetic *HMGA2* 3′-UTR mutant (IDT) were performed Ago2 cleavage analyses were incubated with eIF1A in a series of concentrations (0.01μg/μl, 0.1 μg/μl, 0.3 μg/μl) or eIF1A mutants (0.3 μg/μl) at 37°C for 4h in a 10μl reaction volume. The reaction contained 3μg of yeast tRNAs, 25mM HEPES-KOH, *p*H7.5, 50mM potassium acetate, 5mM magnesium acetate, 5mM DTT, 0.1μl (1μg/μl) native HEK293 cell lysates, 100μM let-7a and linearized 5μM 5′-^{32}P end-labeled synthetic *HMGA2* 3′-UTR mutant, with/without 0.2 μg/μl Ago2. For the *in vitro* pre-miR-451 cleavage analysis, 5μM of 5′-^{32}P end-labeled synthetic pre-miR-451 (Dharmacon) and 0.2 μg/μl Ago2 were incubated with eIF1A in a series of concentrations (0.01μg/μl, 0.1 μg/μl, 0.3 μg/μl), or eIF1A mutants (V55A, K56A, K67A) (0.3 μg/μl) in a 10 μl reaction volume at 37°C for 4h. The reaction contained 3μg of yeast tRNAs, 25mM HEPES-KOH, *p*H7.5, 50mM potassium acetate, 5mMmagnesium acetate, 5mM DTT, and 0.1μl (1μg/μl) native HEK293 cell lysate. The ethanol precipitated RNAs were analyzed in 4~20% Mini-PROTEAN® TBE Precast Gel (BioRad). The gel was quantified by Phosphorimager analyses.

Endogenous miRNA-guided RISC activity assays

To read miRNA-guided RISC activity, pcDNA-GFP-*let 7* (complementary sequence of miRNA *let-7*, 5′-AACTATACA ACCTACTACCTCA-3′) were generated in HEK293 cells as previously described[36]. The pcDNA-GFP-*let 7* was transfected into HEK293 cells followed by 1.6mg/ml G418 selection for two weeks. The resistant colonies were propagated into stable cell lines. For let-7 RISC activity assay, 2μg of expression constructs were transfected into 5×10^5 cells of the GFP–reporter stable cell lines in six-well plates, the cells were transferred to 10cm plates after 24h. After 36hr, total proteins were extracted with standard RIPA buffer together with protease inhibitor (Roche) and total RNAs were extracted using Trizol reagents (Invitrogen). Control Morpholino (MO) or 62.5μM *eif1axb* MO plus 1μg/μl human *eIF1A* or mutant mRNAs were injected into one-cell stage zebrafish embryos. Total RNAs and proteins were isolated at 48 h.p.f. for the analyses of c-Myb proteins and mRNAs.

Zebrafish *eif1axb* knockdown and mRNA microinjection

The wild type *AB/C32*-strain zebrafish were used in this study. All the experiments were conducted according to US National Institutes of Health guidelines for animal research and were approved by Harvard Medical Animal Committee. The morpholino targeting +1~+25 of *eif1axb* (5′-CTCCTTTTCCTTTGTTTTTCGGCAT-3′) and control morpholino (5′-

CCTCTTACCTCA GTTACAATTTATA-3′) were obtained from Gene-Tools. Zebrafish embryos were injected at the one-cell stage with 1nl of 250μM control, 250μM *eif1axa*, 250μM *eif1axb*, 125μM *eif1axb* and combined 125μM *eif1axa*+125μM *eif1axb* morpholino with a PLI-100A Pico-Injector. Images were taken at 19 h.p.f, 28 h.p.f. and 45h.p.f.

Total RNAs and proteins were extracted for microRNA, quantitative real-time PCR (qPCR) and Western blot assays. Antibodies of anti-Ago2 (ab57113, monoclonal), anti-eIF1A (ab38976, polyclonal), and anti-c-Myb (ab62824, polyclonal) ordered from Abcam were used in zebrafish western blot assays. Antibodies of anti-β-actin (#4967, polyclonal) were ordered from Cell Signaling. The qPCR assays were performed with primers (forward and backward): 5′-GAACGGCATCAAGGTGAACTT-3′ and 5′-GACGACCTCGAGTGAGGTAGTAGGTTG TATA-3′ for GFP-let-7; 5′-AAATCTGGCACCACACCTTCTAC-3′ and 5′-GATAGCACA GCCTGGATAGCAAC-3′ for human β-actin; 5′-GCATCATGGTTCTGAAGACTGG-3′ and 5′-CTTCTGCACCAACTCAATCACC-3′ for c-Myb; 5′-GACCCAGACATCAGGGAGT GAT-3′ and 5′-ATGCCAGATCTTCTCCATGTCA-3′ for zActin; 5′-CCAGGATGTCAAA GCAGATGTC-3′ and 5′-ATGTCGTCATCGTTCTCTCCAA-3′ for eif1axa; 5′-TCATCAAG ATGTTGGGAAATGG-3′ and 5′-CCTAGCCTCGTCGGCATTATAC-3′ for eif1axb.

Northern blot assays

Total RNAs were isolated from HEK293 cells, stable HEK293 cells expressing eIF1Amutants (V55A, K56A, or K67A), and developing zebrafish with Trizol (Invitrogen). 25μg total RNAs were loaded into each well of TBE precast gel (Bio-Rad). Northern blot experiments were performed with semi-dry transfer cell and 5′-^{32}P labeled probes. The mature miR-451 and miR-144 specific probes sequences are: 5′-AACUCAGUAAUGGUAACGGUUU-3′ for miR-451; 5′-AGUACAUCAUCUAUACU GUA-3′ for miR-144. U6 probe: 5′-AAAAAUAUGGAACGC UUCACGAAUUUG-3′ for U6 (probes were ordered from IDT).

Taqman real-time PCR

Mature miRNA specific Taqman real-time PCR were performed as TaqMan® manufacture (Taqman microRNA reverse transcription Kit, TaqMan® Universal Master Mix II, no UNG Mini-Pack, and TaqMan® Small RNA Assay) described with the following sequences: let-7(5′-UGAGGUAGUAGGUUGUAUAGUU-3′), miR-126(5′-UCGUAC CGUGAGUAAUAAUGC-3′). Data were normalized to let-7 in zebrafish samples and calculated as manufacture described. The standard deviations were obtained from three independent experiments.

mRNA preparation and rescue analyses

The pCS2Flag constructs (pCS2Flag-vector from Addgene, 16331#) harboring genes encoding human eIF1A or eIF1A (K56A) were linearlized with ApaI restriction enzyme. The mRNAs were prepared with mMESSAGE mMACHINE® SP6 Kit (Invitrogen) following the manufacturer's instructions. The mRNAs were purified with RNeasy Plus Mini Kit (Qiagen) with RNase-free H_2O. Rescue of the *eif1axb* MO (62.5μM, 1nl)

introduced zebrafish was performed by injection of 1000pl of a 1μg/μl mRNA encoding human eIF1A or eIF1A (K56A) into wild type one-cell-stage zebrafish embryos. Experiments with injection of 1000pl of *eif1axb* MO (62.5μM) plus 1μg/μl mRNA encoding human eIF1A (K56A) and 0.2 μg/μl miR-451(IDT) were performed.

Site-directed mutagenesis

The pfu-PCR assays for the site-directed mutagenesis of V55A, K56A and K67A of HA-tagged human eIF1A were performed with the following primers: V55A: Sense: 5′-GCAATGTGTTTCGATGGTGCAAAGAGGTTATGTC ACATC-3′; Antisense: 5′-GATGTGACATAACCTCTTTGCACCATCGAAACACATT GC-3′; K56A: Sense: 5′-GAAGCAATGTGTTTCGATGGTGTAGCGAGGTTATGTCA CATCAG-3′; Antisense: 5′-CTGATGTGACATAACCTCGCTACACCATCGAAACACATTGCTTC-3′; K67A: Sense: 5′-GTCACATCAGAGGAAAATTGAGAGCAAAGGTTTGGATAAATA CCTCGG-3′; Antisense: 5′-CCGAGGTATTTATCCAAACCTTTG CTCTCAATTTTCCTCTG ATGTGAC-3′. The reactions in volume of 10μl of each with sense primers or antisense primers were separately performed pfu-PCR with procedures: 1) 95°C, 3 minutes; 2) 95°C, 20 seconds; 3) 65°C 20seconds; 4) 72°C, 5–12 minutes; 10 cycles (step 2 ~ 4); 5) 72°C, 10 minutes; 6) 4 °C. Combine the sense reaction and antisense reaction products (total volume of 20 μl for each reaction) and continue pfu-PCR with procedures: 1) 95°C, 3 minutes; 2) 95°C, 20 seconds; 3) 65°C 20seconds; 4) 72°C, 5–12 minutes; 20 cycles (step 2 ~ 4); 5) 72°C, 10 minutes; 6) 4 °C. The pfu-PCR products were digested with DpnI restriction enzyme (New England Biolabs) at 37°C for 2hr. The DNAs were transformed into Z-Competent™ E. Coli Cells-Strain Zymo 5α (Zymo Research). Constructs, which were validated by sequencing, harboring correct sequences encoding HA-tagged eIF1A (V55A), eIF1A (K56A) and eIF1A (K67A) were used in this study.

Polysome Profiling

Growth medium was aspirated and cells were washed with PBS, recovered in lysis buffer (50 mM HEPES/KOH pH 7.5, 100 mM NH_4Cl, 25 mM $MgCl_2$, 1 mM DTT, 0.5% (w/v) Triton X-100) and passed 6x through a 27-gauge needle. Insoluble material was removed by a 3-minute spin (microcentrifuge, 20817 rcf). All steps during sample preparation were done on ice or at 4°C. ≈ 100 μl of the lysates (corresponding to ≈ 2×10^6 cells) were loaded onto linear sucrose density gradients (10–40% (w/v) sucrose in lysis buffer) and centrifuged for 2h at 40000 rpm (SW40 rotor, Beckman Coulter) at 4 °C. The gradients were fractionated on a Piston Gradient Fractionator (BioComp Instruments, Fredericton, Canada) and ribosome profiles were recorded at 260 nm.

In Vitro Translation Assays

The dicistronic reporter construct, containing the Renilla luciferase sequence after the 5′ UTR followed by the CrPV IRES and the firefly luciferase sequence, has been previously described[42]. The reporter construct plasmid was linearized with Bam*HI* (New England Biolabs) and transcribed *in vitro* with an ARCA cap and poly (A)-tailed using the mMessage Machine T7 Ultra Kit (Ambion). The mRNAs were purified with RNeasy Plus Mini Kit (Qiagen) with RNase-free H_2O. Human eIF1A and mutants (V55A, K56A and K67A, with

anti-Flag antibodies, 0.15mg/ml, 2μl per reaction per reaction) were purified with Dyna beads (Invitrogen) from HEK293 cells with transient transfection of plasmids encoding Flag-tagged eIF1A and eIF1A mutants. In vitro translation reactions (50μl per reaction) were carried out using Rabbit Reticulocyte Lysate (Promega, 35μl per reaction) with 2mM magnesium acetate and 60mM potassium acetate, which was incubated at 30°C for 100 min. Translation of the reporter genes was measured using the Dual-Glo luciferase assay (Promega). Three independent experiments were performed.

O-Dianisidine staining

O-dianisidine (Sigma) solution at 0.7 mg/ml was prepared in fresh ethanol and protected from exposure to light. The staining solution was prepared by mixing 2 ml of water, 2 ml of 0.7 mg/ml O-dianisidine solution, 0.5 ml of 100 mM sodium acetate, and 100 μl 3% hydrogen peroxide. PTU treated 48 h.p.f embryos were transferred to 12-well plates and 1 ml of the staining solution was added. Stained embryos were kept in the dark for 15 minutes, washed three times with 1 × PBS, and fixed with 4% paraformaldehyde.

May-Grünwald/Giemsa staining

Erythrocytes collection of 20 zebrafish (56 h.p.f) of each group was performed by cutting the zebrafish tails. Circulating erythrocytes were collected with 1 × PBS with 10% FBS with cytospin. The erythrocytes on slides were stained with May-Grünwald/Giemsa solutions (Polysciences), imaged and photographed using a Nikon 80i Upright Microscope. The pixel area of the nucleus and cytoplasm was quantified for 100–145 cells per sample in three independent experiments using ImageJ software and the nuclear: cytoplasmic ratio calculated for each cell.

Image acquisition

In O-Dianisidine staining assays, stained embryos were imaged and photographed using a Leica M80 Microscope with a Nikon D200 digital camera using an adjustable flash system. Erythrocytes with May-Grünwald/Giemsa staining were imaged by Nikon 80i Upright Microscope in Nikon Image Center at Harvard Medical School. Fluorescence and/or DAPI stained images were taken with a Nikon Ti Inverted Fluorescence Microscope with Perfect Focus System in Nikon Image Center at Harvard Medical School. Images of zebrafish embryos were taken by a Leica M80 Microscope with a Nikon D200 digital camera.

Statistical analyses

All statistical experimental data are presented as mean ± s.d. (n = 3 or more). *P*-value was determined by Student's *t*-test (tail = 2). *** $p < 0.01$.

Supplementary Material

Refer to Web version on PubMed Central for supplementary material.

Acknowledgments

We are grateful for support from NIH (grants CA068262, GM047467) and the Agilent Foundation. For technical support and expertise we thank the Nikon Imaging Center and the Institute of Chemistry and Cell Biology (ICCB)

of Harvard Medical School, Charles Richardson, Yang Shi, Steven Elledge, Leonard Zon and Stephen Buratowski. We thank Qikai Xu for the helpful discussion during the early stage of the project.

References

1. Borchert GM, Lanier W, Davidson BL. RNA polymerase III transcribes human microRNAs. Nat Struct Mol Biol. 2006; 13:1097–1101. [PubMed: 17099701]
2. Lee Y, et al. MicroRNA genes are transcribed by RNA polymerase II. EMBO J. 2004; 23:4051–4060. [PubMed: 15372072]
3. Denli AM, Tops BB, Plasterk RH, Ketting RF, Hannon GJ. Processing of primary microRNAs by the Microprocessor complex. Nature. 2004; 432:231–235. [PubMed: 15531879]
4. Gregory RI, et al. The Microprocessor complex mediates the genesis of microRNAs. Nature. 2004; 432:235–240. [PubMed: 15531877]
5. Lund E, Guttinger S, Calado A, Dahlberg JE, Kutay U. Nuclear export of microRNA precursors. Science. 2004; 303:95–98. [PubMed: 14631048]
6. Yi R, Qin Y, Macara IG, Cullen BR. Exportin-5 mediates the nuclear export of pre-microRNAs and short hairpin RNAs. Genes Dev. 2003; 17:3011–3016. [PubMed: 14681208]
7. Gregory RI, Chendrimada TP, Cooch N, Shiekhattar R. Human RISC couples microRNA biogenesis and posttranscriptional gene silencing. Cell. 2005; 123:631–640. [PubMed: 16271387]
8. Maniataki E, Mourelatos Z. A human, ATP-independent, RISC assembly machine fueled by pre-miRNA. Genes Dev. 2005; 19:2979–2990. [PubMed: 16357216]
9. MacRae IJ, Ma E, Zhou M, Robinson CV, Doudna JA. In vitro reconstitution of the human RISC-loading complex. Proc Natl Acad Sci U S A. 2008; 105:512–517. [PubMed: 18178619]
10. Ota H, et al. ADAR1 forms a complex with Dicer to promote microRNA processing and RNA-induced gene silencing. Cell. 2013; 153:575–589. [PubMed: 23622242]
11. Chendrimada TP, et al. TRBP recruits the Dicer complex to Ago2 for microRNA processing and gene silencing. Nature. 2005; 436:740–744. [PubMed: 15973356]
12. Hutvagner G, et al. A cellular function for the RNA-interference enzyme Dicer in the maturation of the let-7 small temporal RNA. Science. 2001; 293:834–838. [PubMed: 11452083]
13. Ketting RF, et al. Dicer functions in RNA interference and in synthesis of small RNA involved in developmental timing in C. elegans. Genes Dev. 2001; 15:2654–2659. [PubMed: 11641272]
14. Cheloufi S, Dos Santos CO, Chong MM, Hannon GJ. A dicer-independent miRNA biogenesis pathway that requires Ago catalysis. Nature. 2010; 465:584–589. [PubMed: 20424607]
15. Cifuentes D, et al. A novel miRNA processing pathway independent of Dicer requires Argonaute2 catalytic activity. Science. 2010; 328:1694–1698. [PubMed: 20448148]
16. Yang JS, et al. Conserved vertebrate mir-451 provides a platform for Dicer-independent, Ago2-mediated microRNA biogenesis. Proc Natl Acad Sci U S A. 2010; 107:15163–15168. [PubMed: 20699384]
17. Yoda M, et al. Poly(A)-specific ribonuclease mediates 3′-end trimming of Argonaute2-cleaved precursor microRNAs. Cell Rep. 2013; 5:715–726. [PubMed: 24209750]
18. Doench JG, Petersen CP, Sharp PA. siRNAs can function as miRNAs. Genes Dev. 2003; 17:438–442. [PubMed: 12600936]
19. Liu J, et al. Argonaute2 is the catalytic engine of mammalian RNAi. Science. 2004; 305:1437–1441. [PubMed: 15284456]
20. Meister G, et al. Human Argonaute2 mediates RNA cleavage targeted by miRNAs and siRNAs. Mol Cell. 2004; 15:185–197. [PubMed: 15260970]
21. Petersen CP, Bordeleau ME, Pelletier J, Sharp PA. Short RNAs repress translation after initiation in mammalian cells. Mol Cell. 2006; 21:533–542. [PubMed: 16483934]
22. Humphreys DT, Westman BJ, Martin DI, Preiss T. MicroRNAs control translation initiation by inhibiting eukaryotic initiation factor 4E/cap and poly(A) tail function. Proc Natl Acad Sci U S A. 2005; 102:16961–16966. [PubMed: 16287976]
23. Bartel DP. MicroRNAs: target recognition and regulatory functions. Cell. 2009; 136:215–233. [PubMed: 19167326]

24. Song JJ, Smith SK, Hannon GJ, Joshua-Tor L. Crystal structure of Argonaute and its implications for RISC slicer activity. Science. 2004; 305:1434–1437. [PubMed: 15284453]
25. Frank F, Sonenberg N, Nagar B. Structural basis for 5′-nucleotide base-specific recognition of guide RNA by human AGO2. Nature. 2010; 465:818–822. [PubMed: 20505670]
26. Yan KS, et al. Structure and conserved RNA binding of the PAZ domain. Nature. 2003; 426:468–474. [PubMed: 14615802]
27. Parker JS, Roe SM, Barford D. Structural insights into mRNA recognition from a PIWI domain-siRNA guide complex. Nature. 2005; 434:663–666. [PubMed: 15800628]
28. Ma JB, et al. Structural basis for 5′-end-specific recognition of guide RNA by the A. fulgidus Piwi protein. Nature. 2005; 434:666–670. [PubMed: 15800629]
29. Elkayam E, et al. The Structure of Human Argonaute-2 in Complex with miR-20a. Cell. 2012; 150:100–110. [PubMed: 22682761]
30. Schirle NT, MacRae IJ. The crystal structure of human Argonaute2. Science. 2012; 336:1037–1040. [PubMed: 22539551]
31. Battiste JL, Pestova TV, Hellen CU, Wagner G. The eIF1A solution structure reveals a large RNA-binding surface important for scanning function. Mol Cell. 2000; 5:109–119. [PubMed: 10678173]
32. Yu Y, et al. Position of eukaryotic translation initiation factor eIF1A on the 40S ribosomal subunit mapped by directed hydroxyl radical probing. Nucleic acids research. 2009; 37:5167–5182. [PubMed: 19561193]
33. Hussain T, et al. Structural changes enable start codon recognition by the eukaryotic translation initiation complex. Cell. 2014; 159:597–607. [PubMed: 25417110]
34. Iwasaki S, et al. Hsc70/Hsp90 chaperone machinery mediates ATP-dependent RISC loading of small RNA duplexes. Mol Cell. 2010; 39:292–299. [PubMed: 20605501]
35. Mayr C, Hemann MT, Bartel DP. Disrupting the pairing between let-7 and Hmga2 enhances oncogenic transformation. Science. 2007; 315:1576–1579. [PubMed: 17322030]
36. Qi HH, et al. Prolyl 4-hydroxylation regulates Argonaute 2 stability. Nature. 2008; 455:421–424. [PubMed: 18690212]
37. Grabher C, et al. Zebrafish microRNA-126 determines hematopoietic cell fate through c-Myb. Leukemia. 2011; 25:506–514. [PubMed: 21079614]
38. Dore LC, et al. A GATA-1-regulated microRNA locus essential for erythropoiesis. Proc Natl Acad Sci U S A. 2008; 105:3333–3338. [PubMed: 18303114]
39. Pase L, et al. miR-451 regulates zebrafish erythroid maturation in vivo via its target gata2. Blood. 2009; 113:1794–1804. [PubMed: 18849488]
40. Ameres SL, et al. Target RNA-directed trimming and tailing of small silencing RNAs. Science. 2010; 328:1534–1539. [PubMed: 20558712]
41. Kawamata T, Tomari Y. Making RISC. Trends Biochem Sci. 2010; 35:368–376. [PubMed: 20395147]
42. Moerke NJ, et al. Small-molecule inhibition of the interaction between the translation initiation factors eIF4E and eIF4G. Cell. 2007; 128:257–267. [PubMed: 17254965]
43. Yang JS, Lai EC. Alternative miRNA biogenesis pathways and the interpretation of core miRNA pathway mutants. Mol Cell. 2011; 43:892–903. [PubMed: 21925378]

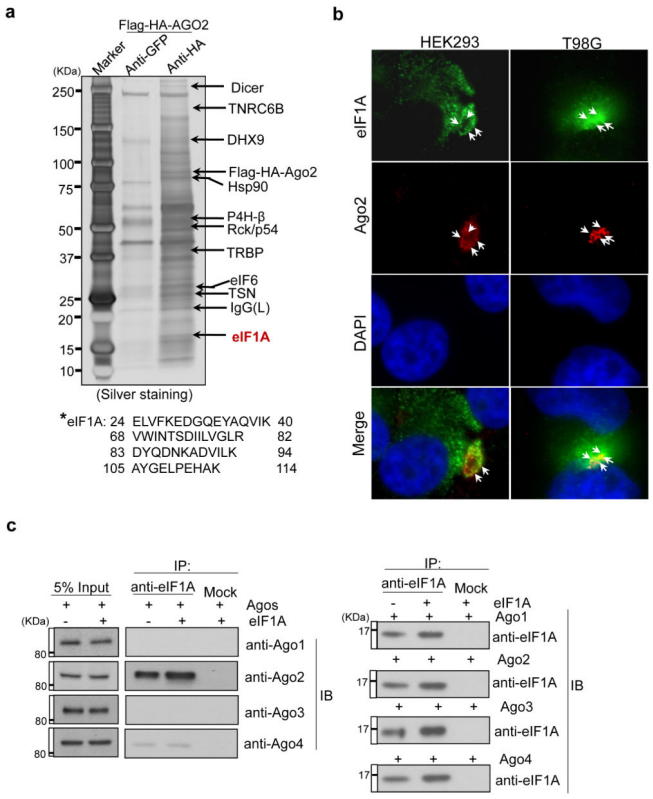

Figure 1. eIF1A interacts with Ago2

(**a**) Proteins co-immunoprecipitated with Flag-HA-Ago2 from HEK293 cells were separated by SDS-PAGE (silver staining) and analyzed by mass spectrometry. eIF1A is a novel Ago2 interacting protein (*:detected peptides of eIF1A). (**b**) Fluorescence immunostaining was performed with anti-eIF1A (monoclonal) and anti-Ago2 (monoclonal) antibodies and DAPI (4′,6-diamidino-2-phenylindole) in HEK293 and human glioblastoma multiforme T98G cells. White arrows show the co-localized eIF1A and Ago2. (**c**) eIF1A interacts with Ago2. Human *eIF1A* was transiently overexpressed in stable HEK293 cells stably expressing Agos (1~4). Immunoprecipitation assays were performed with anti-eIF1A (monoclonal) antibody and immuno blotting (IB) with anti-Agos antibodies in the upper panel and anti-eIF1A antibodies in the bottom panel.

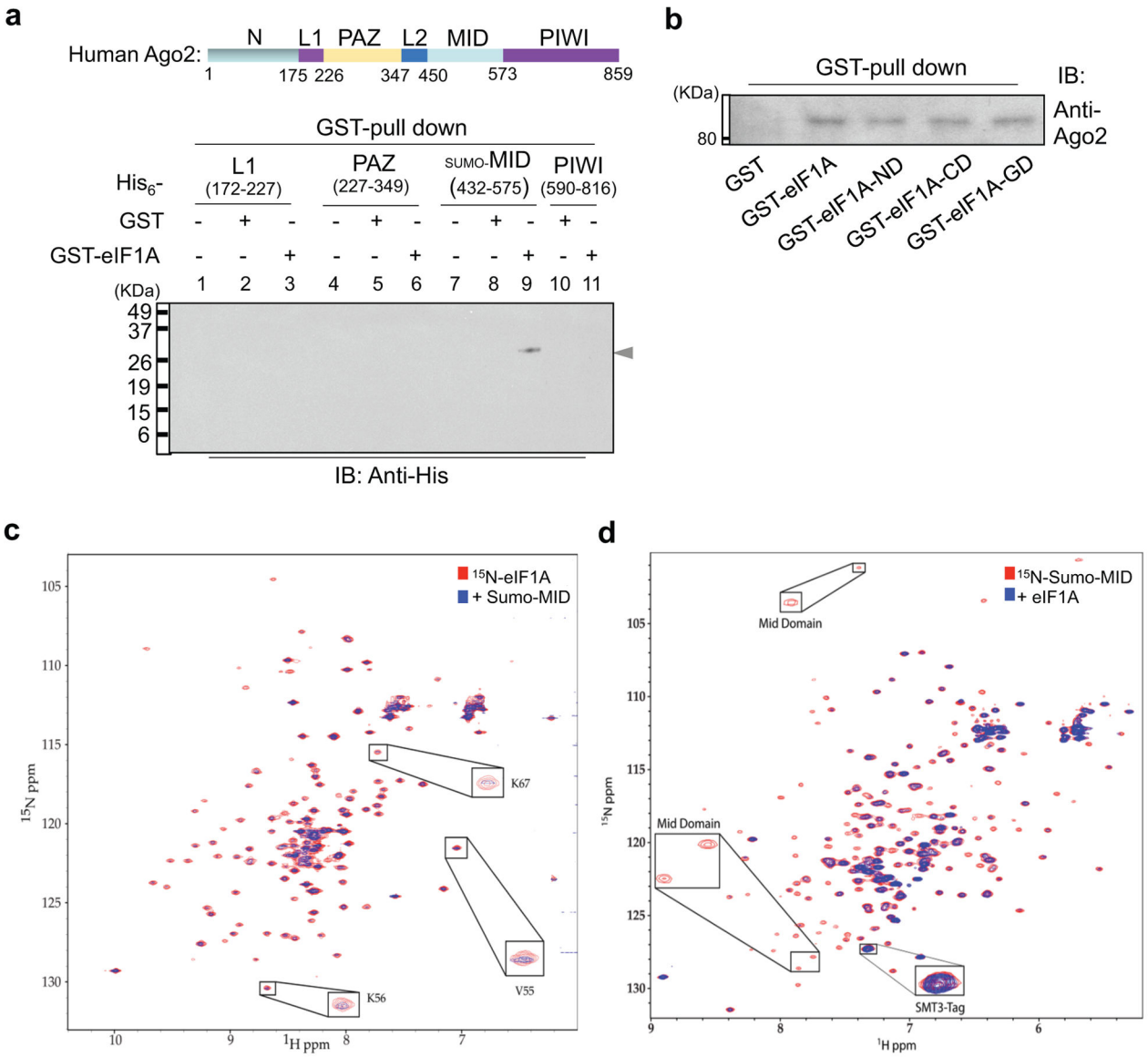

Figure 2. eIF1A binds to MID-domain of Ago2 in a RNA-binding-independent manner

(**a**) Human eIF1A interacts with the MID fragment of human Ago2. Recombinantly expressed and Benzonase-treated Ago2 fragments and recombinantly expressed GST-eIF1A were used for GST-pull down analyses followed by Western blotting with anti-His antibodies (IB, immuno-blotting). The arrow shows that the MID fragment interacts with eIF1A. (**b**) The globular domain (GD) of eIF1A interacts with Ago2. Recombinantly expressed and Benzonase-treated GST, GST-eIF1A and mutants (ND, 25 ~ 144aa; CD, 1 ~ 114aa; GD, 25 ~ 114aa) were used for GST-pull down assays with cell lysates of HEK293 stably expressing Ago2. (**c**) ^{1}H-^{15}N TROSY-HSQC spectrum of ^{15}N-eIF1A titrated with the sumo-MID (432 ~ 575aa). The titration of RNA-free-sumo-MID leads to broadening of RNA free ^{15}N-eIF1A resonances (molar ratio of 1:1). Inserted frames show the broadening of resonances of V55, K56 and K67 residues in eIF1A upon MID titration. (**d**) ^{1}H-^{15}N TROSY-HSQC spectrum of ^{15}N-Sumo-MID titrated with eIF1A. The titration of eIF1A

(molar ratio of 1:1) results in broadening ^{1}H-^{15}N TROSY-HSQC crosspeaks coming from the ^{15}N-MID domain, but not from ^{15}N-Sumo (SMT3) tag. Inserted frames show the broadening of resonances of residues from MID-domain, but not from SMT3-Tag (SUMO-tag), upon eIF1A titration.

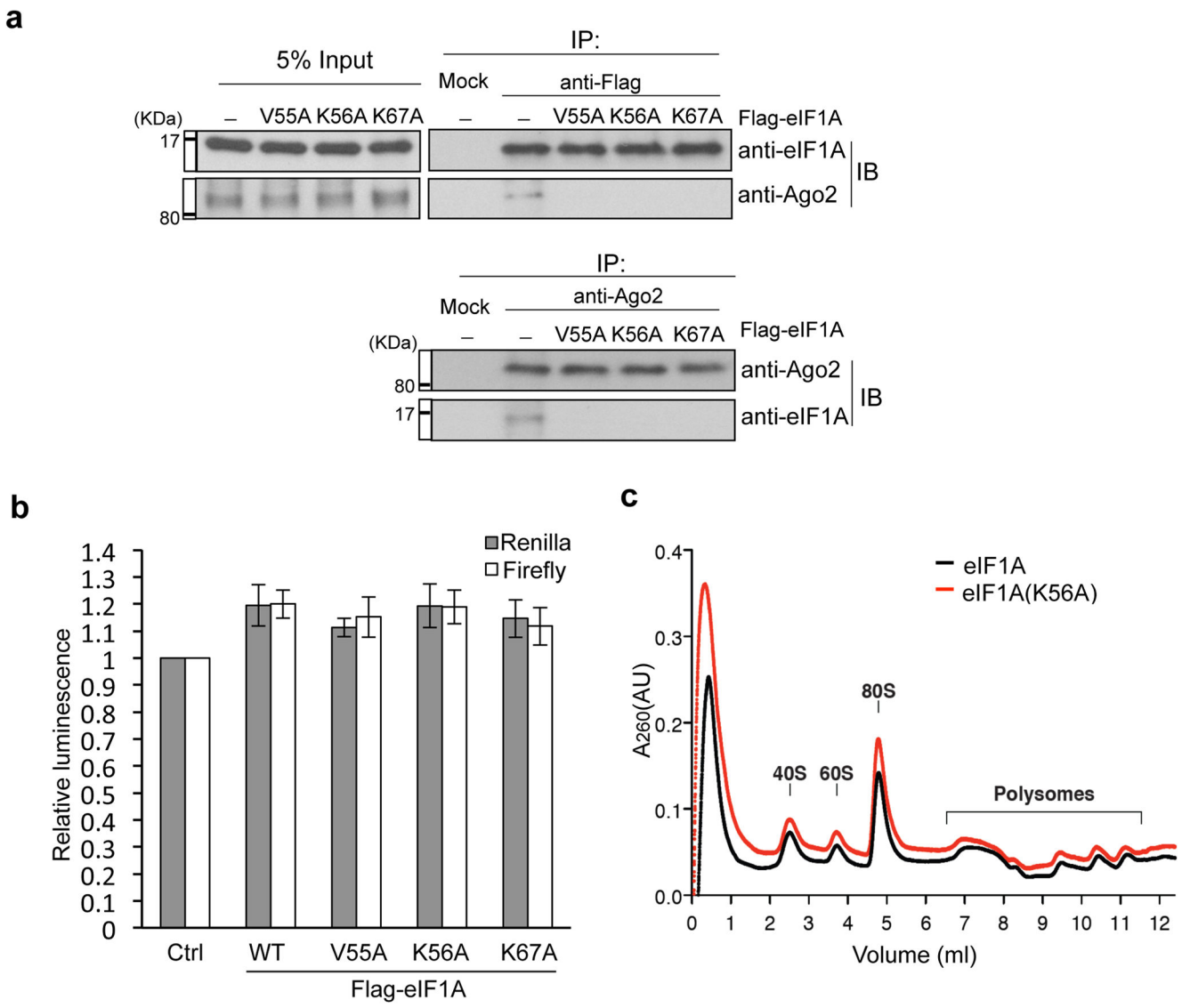

Figure 3. Lys56 in eIF1A is important for full length eIF1A-Ago2 interaction but K56A mutation in eIF1A does not impair translation initiation

(**a**) Immunoprecipitation (IP) assays were performed with and anti-Flag antibodies in HEK293 cell lines stably expressing Flag-tagged eIF1A and eIF1A mutants. Bottom panel: immunoprecipitation assays were performed with anti-Ago2 antibodies. Immunoblotting (IB) assays were performed with anti-eIF1A and anti-Ago2 antibodies. (**b**) 0.3μg added purified Flag-eIF1A (K56A) mutants per reaction display the similar promotion effects as 0.3μg added purified Flag-eIF1A and Flag-eIF1A mutants per reaction in cap-dependent and IRES-dependent translation in dual luciferase assays *in vitro*. Relative luminescence results were shown. Three independent experiments were performed (mean ± s.d., n = 3). (**c**) Polysome profiling analyses with HEK293 cell lines stably expressing eIF1A or eIF1A (K56A). Extracts of the indicated cell lines were subjected to sucrose density gradient centrifugation. The ribosome profiles (recorded at 260 nm) and the positions of the 40S/60S ribosomal subunits, 80S monosome and polyribosomes are shown.

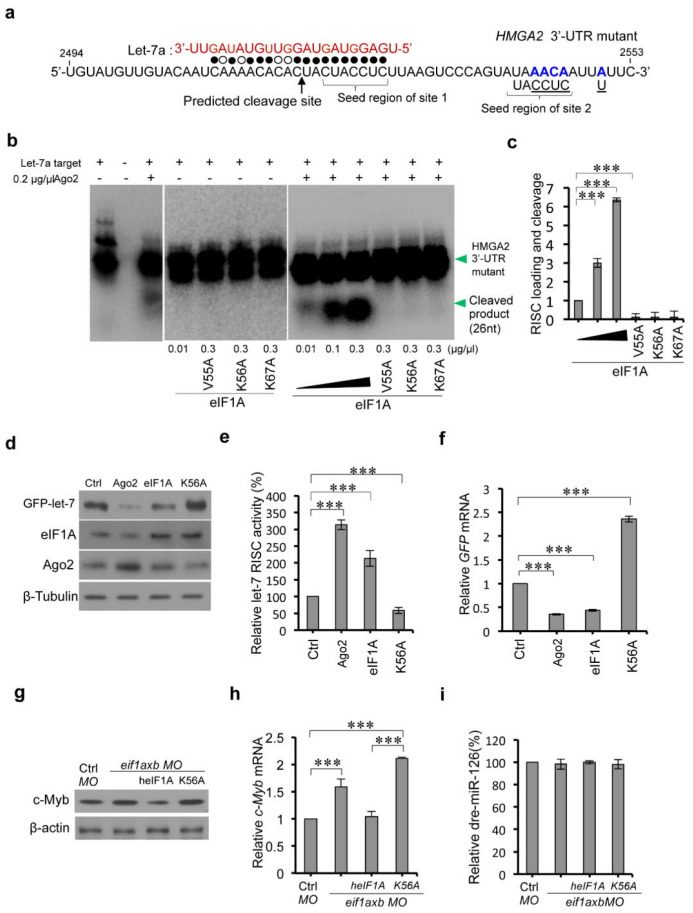

Figure 4. eIF1A augments Ago2-mediated RNAi

(**a**) Sequence of the human *HMGA2* 3′-UTR fragment mutant with two native let-7 target sites. Filled circles: Watson-Crick complementarity; open circles: non-Watson-Crick complementarity. Mutated nucleotides are shown in blue and wild type nucleotides were underlined (to neutralize site 2 and to reduce self-complementarity). (**b**) *In vitro* effects of eIF1A on Ago2-mediated RNA cleavage. eIF1A or the indicated mutants were incubated with Ago2, synthetic let-7a and 5′-^{32}P end-labeled *HMGA2* 3′-UTR mutants. RNAs were analyzed by Northern blot and autoradiographs analyses. (**c**) Statistical analyses of three independent *in vitro* assays in (**b**). (**d**) Western blot assays of effects of eIF1A and eIF1A (K56A) mutant on GFP-let-7 reporter expression. Ago2, eIF1A or eIF1A (K56A) were transiently overexpressed in HEK293 cells stably expressing reporter GFP-let-7. (**e**)The expression ratio between Tubulin and GFP reporter in the same gel were calculated. Intact (100%) RISC activity was considered in control cells. The relative RISC activities under overexpression conditions of the indicated genes or mutants were obtained by comparison with the control. (**f**) Relative *GFP* reporter mRNAs in (**d**) by quantitative real-time PCR (qPCR). (**g**) Western blot assays of zebrafish c-Myb in the indicated zebrafish groups at 28 h.p.f (control, *eif1axb* MO (62.5μM, 1nl), *eif1axb* MO (62.5μM, 1nl) plus human eIF1A (heIF1A) (mRNA, 1μg/μl, 1000pl), and *eif1axb* MO (62.5μM, 1nl) plus heIF1A (K56A) mutant (mRNA, 1μg/μl, 1000pl)). Proteins were extracted from >10 zebrafish per group. (**h**)

Relative *c-Myb* mRNAs in each group in (**g**) by qPCR. Total RNAs were extracted from >10 zebrafish per group. (**i**) Taqman PCR assays of relative zebrafish miR-126 (dre-miR-126) in each group in (**g**). Total RNAs were extracted from >10 zebrafish per group. In all statistical comparisons, three independent experiments were performed (mean ± s.d., n = 3 experiments, Student's *t*-test). *** reports $p < 0.01$.

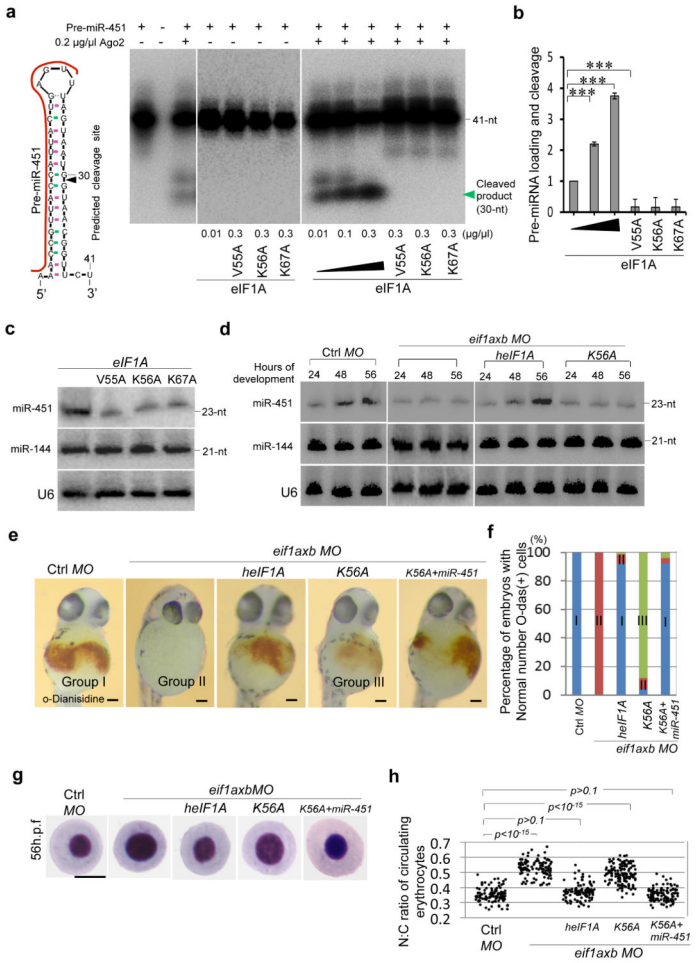

Figure 5. eIF1A augments miR-451 biogenesis

(**a**) *In vitro* activity of eIF1A in Ago2-mediated cleavage of 5′-^{32}P end-labeled synthetic pre-miR-451. RNAs were analyzed by Northern blotting and autoradiographs analyses. (**b**) Statistical analyses of the data in (**a**). Data of three independent experiments were shown (mean ± s.d., n = 3, Student's *t*-test). (**c**) Northern blot assays show the effects of eIF1A mutants on miR-451 biogenesis in HEK293 cells. Total RNAs were extracted from stable HEK293 cells expressing Flag-eIF1A and Flag-eIF1A mutants. Signals show mature miR-451 and miR-144 levels with U6 as a loading control. (**d**) Northern blot assays show the effects of eIF1A(K56A) mutant on miR-451 generation in the developing zebrafish. Total RNAs were extracted from zebrafish with/without treatments of control MO, *eif1axb* MO (62.5μM, 1nl), *eif1axb* MO (62.5μM, 1nl) plus heIF1A (mRNA, 1μg/μl, 1nl), *eif1axb* MO (62.5μM, 1nl) plus heIF1A (K56A) (mRNA, 1μg/μl, 1nl). (**e**) Hemoglobin (brown) was visualized by the oxidation of o-dianisidine (o-das) in zebrafish at 48 h.p.f. Hemoglobinized cells accumulate in wild type (Group I) and are reduced in *eif1axb* MO injected embryos (Group II). Human eIF1A, but not K56A mutant (Group III, with less hemoglobinized cells), rescues hemoglobinized cells in *eif1axb* MO-injected zebrafish, while miR-451 spares K56A caused rescue defects. Scale bar = 100μm. (**f**) Percentage of embryos with hemoglobinized cells in zebrafish. Control group (n=40). *eif1axb* MO injection (n = 42). Human eIF1A (n =

35), but not K56A mutant (n = 35), increased the percentage of embryos with normal hemoglobinized cells, while miR-451 (n = 31) suppresses the decreased percentage by K56A mutant ($p < 0.001$). (**g**) Erythrocytes stained with May-Grünwald/Giemsa are representative of the mean of each group at 56 h.p.f. Scale bar = 5μm. (**h**) Scatterplot of the nuclear cytoplasmic ratio (N:C) for each group as readout of erythrocyte maturation (Wilcoxonrank-sumtest after Bonferroni correction, $p < 10^{-15}$). Human eIF1A (n = 120 erythrocytes), but not K56A mutant (n = 145), rescued erythrocyte maturation impaired by *eif1axb* MO injection, while miR-451(n = 118) spares distribution difference in heIF1A(K56A) mutant group. ***$p < 0.01$.

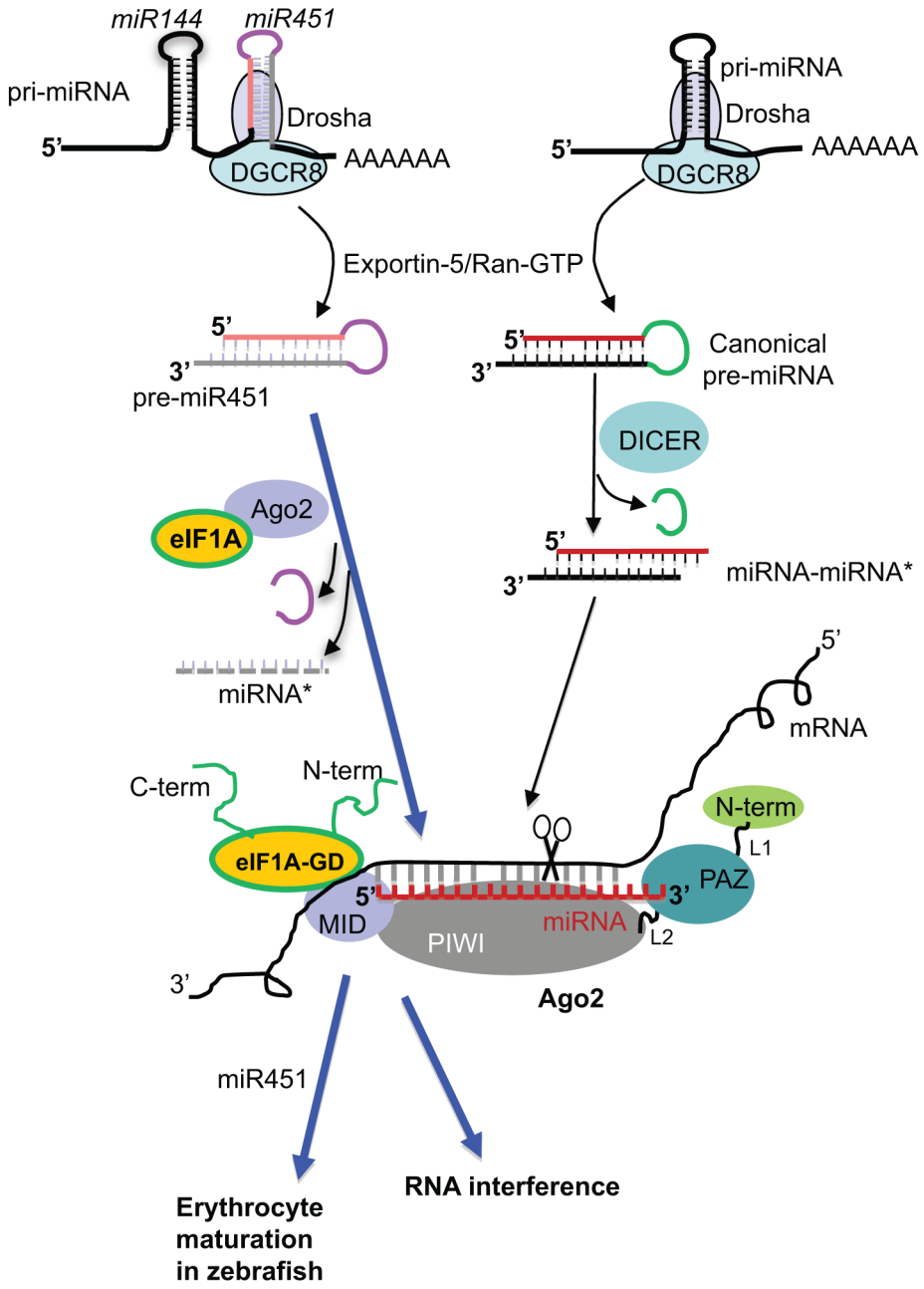

Figure 6. Schematic diagram for eIF1A functions in Ago2-dependent miR-451 biogenesis, RNA interference and erythrocyte maturation in zebrafish

The primary miRNA (priRNA) is cleaved by Drosha-DGCR8 pathways to generate pre-miRNA within the nucleus. Exportin-5 in complex with Ran-GTP exports the pre-miRNA to the cytoplasm, where the pre-miRNA is bound by DICER to form a RISC Loading Complex that includes Ago2. In the canonical miRNA biogenesis pathway, DICER removes the terminal loop region to yield the mature miRNA. The pre-miR-451 is loaded directly onto Ago2 and sliced on the 3′ hairpin arm. The miR-144 biogenesis is DICER-dependent. The globular domain (GD) of eIF1A directly binds to MID-domain of Ago2 and forms an eIF1A-Ago2 complex promoting Ago2-mediated RNAi and miR-451 biogenesis. MID-

domain of Ago2 binds to the GD of eIF1A and does not impair eIF1A functions in translation initiation. The 5′-term of guide strand of miRNA-miRNA* duplex is docked onto a pocket with residues mainly from MID-domain. The long and structured mRNAs are scanned by RISCs to recognize seed regions in miRNAs. After perfect or imperfect complementary guide with miRNAs, mRNAs are nicked by PIWI domain resulting in RNAi. eIF1A augments Ago2-mediated RNAi, miR-451 production and erythrocyte maturation. *Black arrows* are from previous reports of other groups[14,15,43]; *blue arrows* are from this study.